

Towards the optimization of a NLRP3 inflammasome model system in J774A.1 murine macrophages and THP-1 human monocytes

Ali Reza Nasser, Darius Parmar, Mehdi Tabesh, and Junqin Wang

Department of Microbiology and Immunology, University of British Columbia, Vancouver, British Columbia, Canada

SUMMARY The NLRP3 inflammasome is a cytosolic, multimeric protein complex, that detects and responds to modulations in tissue homeostasis disruptions such as pathogen detection, tissue damage, and environmental stressors. Dysregulated NLRP3 inflammasome activity has been linked to various autoinflammatory and autoimmune diseases including diabetes and Alzheimer's disease, rendering the inflammasome an attractive potential therapeutic target. However, NLRP3 activation mechanisms are complex and can be induced by a multitude of stimulatory conditions, leading to challenges with developing a reliable model system. In this study, we aimed to optimize appropriate conditions to detect NLRP3 inflammasome activation in both J774A.1 murine macrophages and THP-1 human monocytes. In J774A.1 cells, we detected upregulated expression of pro-IL-1 β following LPS-treatment, indicative of NLRP3 inflammasome priming. Following nigericin stimulation, we observed diminished pro-IL-1 β levels and no mature IL-1 β . We were able to differentiate THP-1 monocytic cells into macrophage-like phenotypes using 500nM PMA treatment for 24 hours. Following nigericin treatment, ASC levels decreased in LPS-undifferentiated, and increased in PMA-differentiated THP-1 cells relative to their respective untreated controls. We observed nigericin-induced, duration-dependent increases in cell death for both THP-1 phenotypes using a cell viability assay. In conclusion, we confirmed prior findings regarding J774A.1 NLRP3 inflammasome signaling and initiated the optimization of NLRP3 inflammasome activation in THP-1 cells. Further enhancements are required to conclusively identify NLRP3 activation and optimize a reliable cell line model system.

INTRODUCTION

To initiate an immune response, cells of the innate immune system possess pattern recognition receptors (PRR) to detect pathogen associated molecular patterns (PAMPs) and damage associated molecular patterns (DAMPs). The innate immune system needs to be responsive to PAMPs and DAMPs as these molecules indicate disrupted tissue homeostasis, and can originate from microorganisms, environmental stressors, and/or tissue damage (1). One cellular mechanism used to respond to PAMPs and DAMPs are cytosolic multimeric protein complexes known as inflammasomes (2). In particular, the NOD-like receptor family, pyrin domain containing 3 (NLRP3) inflammasome is activated in response to multiple PAMPs and DAMPs (2). The recognition of the PAMP/DAMP is mediated by the NLRP3 protein, an intracellular PRR. The pro-inflammatory activity of the NLRP3 inflammasome is mediated by the apoptosis-associated speck-like protein containing a caspase-recruitment domain (ASC) protein (2). Upon inflammasome oligomerization, the ASC protein allows pro-caspase-1 to associate with the inflammasome complex and become auto-proteolytically cleaved into mature caspase-1 (2). Mature caspase-1 then proteolytically cleaves immature pro-inflammatory cytokines pro-interleukin-1 β (pro-IL-1 β) and pro-IL-18, and pyroptosis-inducing pro-Gasdermin-D (GSDMD) protein. Mature IL-1 β and IL-18 are secreted and provide pro-inflammatory signaling to neighboring cells, propagating the inflammatory immune response (2). GSDMD is cleaved into N-terminal and C-terminal subunits by caspase-1. The GSDMD^{N-term} domain forms pore complexes in the plasma membrane, contributing to the release of pro-inflammatory molecules and inducing pyroptosis (2).

NLRP3 inflammasome activation is thought to occur by a two-step priming and activation process. The priming step involves the detection of PAMPs or DAMPs by cellular PRRs,

Published Online: September 2023

Citation: Nasser, Parmar, Tabesh, Wang. 2023. Towards the optimization of a NLRP3 inflammasome model system in J774A.1 murine macrophages and THP-1 human monocytes. UJEMI 28:1-11

Editor: Lauren Pugsley and Shruti Sandilya, University of British Columbia

Copyright: © 2023 Undergraduate Journal of Experimental Microbiology and Immunology. All Rights Reserved.

Address correspondence to:
<https://jemi.microbiology.ubc.ca/>

which activates nuclear factor kappa B (NF- κ B), inducing transcriptional upregulation of NLRP3 inflammasome components, immature pro-inflammatory cytokines, and pyroptosis-mediators (2, 3). The second signal induces the oligomerization and activation of effector functions of the NLRP3 inflammasome. Oligomerization has two distinct pathways, canonical and non-canonical. In canonical activation, the second signal is provided by the direct stimulation of the NLRP3 protein by cytosolic PAMPs or DAMPs (2, 3). Non-canonical activation involves the activation of caspase-11 (caspase-4/-5 in murine cells) by direct interaction with cytosolic bacterial lipopolysaccharide (LPS) (3).

Normal NLRP3 inflammasome activity is an important mediator of host innate immune responses against bacterial, fungal, and viral infections. Aberrant NLRP3 inflammasome activity is implicated in the pathogenesis of multiple autoimmune and autoinflammatory diseases including: cryopyrin-associated periodic syndromes (CAPS), multiple sclerosis, Alzheimer's disease, atherosclerosis, and type 2 diabetes (4-6). Consequently, the NLRP3 inflammasome has been identified as a potential therapeutic target and is the subject of active research. Pathways of canonical activation are a focus of current NLRP3 inflammasome studies due to the ability of multiple PAMPs and DAMPs to provide the second activation signal. However, the variability in detecting NLRP3 inflammasome effector functions across studies poses a challenge to developing reliable model systems (7). Identification of successful inflammasome activation typically involves the detection of cleaved IL-1 β (8-10). Previous studies have shown IL-1 β detection in J774A.1 murine macrophages after LPS priming and subsequent treatment with either adenosine triphosphate (ATP) or nigericin (11, 12). However, recent studies in the Undergraduate Journal of Experimental Microbiology (UJEMI) were unable to detect mature IL-1 β in J774A.1 cells using similar LPS priming and ATP/nigericin stimulation (13-15). This variation highlights the need for a defined, reproducible cell line model system for NLRP3 inflammasome activation.

To construct a two-step canonical NLRP3 inflammasome activation model system, we chose to investigate both the J774A.1 murine macrophages and THP-1 human leukemia monocytic cells, which have been shown to contain mature IL-1 β after LPS priming and ATP-/nigericin- stimulation (16, 17). Additionally, THP-1 cells can be differentiated towards a macrophage-like phenotype using phorbol 12-myristate 13-acetate (PMA) (18). LPS is a toll-like receptor 4 (TLR4) agonist, which through the NF- κ B pathway, provides the priming signal of NLRP3 inflammasome activation (1-3). Upregulation of pro-IL-1 β is consistently detected following LPS-treatment in J774A.1 cells and undifferentiated THP-1 cells (13-15). For differentiated THP-1 cells, PMA is sufficient to prime the NLRP3 inflammasome. PMA acts as a specific activator of protein kinase C (PKC), which positively contributes to NF- κ B-mediated transcriptional regulation (19). We used ATP and nigericin for the second activation signal. ATP accumulates in the extracellular microenvironment during tissue damage and inflammation, providing DAMP signaling for NLRP3 activation (20). Nigericin is a potassium ionophore toxin isolated from *Streptomyces hygroscopicus* that forms pores in the plasma membrane and provides signaling for NLRP3 inflammasome activation (21).

We hypothesize an upregulation of pro-IL-1 β in J774A.1 cells and detection of cleaved IL-1 β following LPS priming and nigericin or ATP stimulation. In THP-1 cells, we expect to observe elevated ASC expression, and subsequent cell death following prolonged nigericin treatment of LPS-primed, undifferentiated and PMA-differentiated THP-1 cells. We observed the development of activated, multipolar J774A.1 phenotypes in response to LPS priming and nigericin stimulation. However, ATP failed to induce the same level of phenotypic change relative to nigericin. In J774A.1 cells, we detected intracellular pro-IL-1 β following LPS priming, which diminished following Nigericin treatment, and was absent following ATP treatment. We detected ASC protein in untreated THP-1 cells, which decreased in undifferentiated cells and increased in differentiated cells following nigericin treatment. Using a nuclear staining cell viability assay, we qualitatively observed increased THP-1 cell death with prolonged exposure to nigericin, following either LPS priming or PMA-differentiation. Although our results did not conclusively confirm the NLRP3 inflammasome activation, they provide insights into establishing a robust cell line model system to investigate inflammasome-related disorders.

METHODS AND MATERIALS

Reagent Preparation. LPS (*Escherichia coli*; Sigma-Aldrich, Cat no. L4391) stocks used for priming were pre-made at a concentration of 1 mg/mL. ATP (Biobasic) was dissolved in complete media and syringe filtered inside the biosafety cabinet (BSC) before use. Nigericin (EMD Millipore, Cat no. 481990) stocks were prepared in 95% ethanol at a concentration of 5 mg/mL. Phorbol 12-myristate 13-acetate (PMA) stocks were prepared in 5% DMSO at a concentration of 100 mg/mL. All stock solutions were stored at -20°C and further diluted in complete media before use. Triton X-100 lysis buffer was pre-made with 20mM Tris (pH 8.8), 127mM NaCl, 10% glycerol, 1% Triton X-100, 2mM EDTA, and distilled H₂O. Sample loading buffer (4x) for the SDS-PAGE was pre-made using 0.25 M Tris-HCl pH 6.8, 8% SDS, 30% Glycerol, and 0.02% Bromophenol Blue containing 0.3M DTT.

J774A.1 Murine Macrophage Cell Culture and Stimulation. J774A.1 cells obtained from the Kronstad Lab, Michael Smith Laboratories, UBC were cultured in Dulbecco's Modified Eagle Medium (DMEM; ThermoFisher) containing 10% fetal bovine serum (FBS; GibCo™, Thermo Fisher, Cat no. 10438026) and 2 mM GlutaMAX L-glutamine (GibCo™, Thermo Fisher, Cat no. 35050061) and maintained in a 37°C incubator with 5% CO₂. Cells were seeded at a density of 2.0x10⁶ cells/dish in 10 cm tissue culture dishes, incubated for 48 hrs, primed with 0.5 µg/mL LPS for 4 hrs, and stimulated with 5 mM ATP or 10 µM nigericin.

THP-1 Human Monocyte Cell Culture and Stimulation. THP-1 cells obtained from the Finlay Lab, UBC were cultured in suspension using DMEM containing 10% FBS, 2mM GlutaMAX L-glutamine and 2mM MEM Non-essential Amino Acids Solutions (GibCo™, Thermo Fisher, Cat no. 11140050). THP-1 cells were differentiated with 500 nM of PMA for 24 hrs. For Western blot and NucGreen Dead 488 imaging, undifferentiated and differentiated THP-1 cells were seeded in 6-well plates at 1.0x10⁶ cells/well. Undifferentiated cells were primed with 1 µg/mL LPS for 4 hrs and stimulated with 10 µM nigericin. Differentiated THP-1 cells were stimulated with 10 µM nigericin following PMA differentiation. Cells were maintained in a 37°C incubator with 5% CO₂.

SDS-PAGE and Turbo-Transfer. Cells were lysed using Triton X-100 lysis buffer supplemented with one cOmplete protease inhibitor tablet (Sigma Aldrich, Cat no. 05892970001). Bicinchoninic acid assay (BCA) was conducted using the Pierce BCA Protein Assay Kit (ThermoFisher, Cat# 23225) according to the manufacturer's instructions. Polyacrylamide gels (10%) were prepared using TGX Stain-Free™ FastCast™ Acrylamide Kit (BioRad, Cat no. 161-0183) according to the manufacturer's protocol. The Spectra™ Multicolor Broad Range Protein Ladder (ThermoFisher, Cat no. 26634) was used. SDS-PAGE protein separation was conducted at 120V for 45 minutes. Turbo-transfers were performed using the BioRad Trans-Blot Turbo Transfer System onto a Trans-Blot Turbo Mini 0.2 µm PVDF membrane (BioRad, Cat no. #1704156) according to the manufacturer's protocol. Ponceau S images were captured with an iPhone camera.

Western Blots. For pro-IL-1β detection, the membrane was blocked in 5% skim milk in Tris-Buffered Saline with 0.1% Tween 20 (TBS-T) for 1 hr and incubated in anti-IL-1β goat polyclonal primary antibody (1:1000 dilution; R&D, Cat no. AF-401-NA) in 1% skim milk-TBS-T overnight at 4°C. Membrane was subsequently incubated for 1 hr in goat IgG HRP-conjugated secondary antibody (1:15000 dilution; R&D, Cat no. HAF109) in 1% skim milk-TBS-T. For ASC detection, the membrane was blocked in 5% Bovine Serum Albumin (BSA) in TBS-T for 1 hr and incubated in anti-ASC murine monoclonal primary antibody (1:500 dilution; Santa Cruz, Cat no. 111-035-003) in 1% BSA-TBS-T overnight at 4°C. The membrane was then incubated for 1 hour in mouse IgG HRP-conjugated secondary antibody (1:15000 dilution; Invitrogen, Cat no. 31430) in 1% BSA-TBS-T. The membranes were developed using Pierce ECL Western Blotting Substrate (ThermoFisher, Cat# 32106) and visualized using the ChemiDoc MP Imaging System (BioRad). The membranes were washed 3 times for 5 mins each with TBS-T between each step and with TBS prior to imaging.

Cell Viability Fluorescence Microscopy. Cells were stained with NucGreen™ Dead 488 (ThermoFisher, Cat no. R37109) reagent in complete DMEM, incubated for 5 mins, and imaged according to manufacturer’s instructions. Fluorescence and transmitted microscopy images were taken at 10X magnification and processed via ImageJ.

Graphical Quantification and Statistical Analysis. Cellular area and perimeter were manually semi-quantified using ImageJ based on 15 randomly selected cells with a set scale of 225 pixels = 50 µm. Statistical illustrations and tests were conducted via GraphPad Prism.

RESULTS

LPS-primed J774A.1 cells treated with nigericin exhibit greater morphological changes relative to ATP-treated cells, and produce detectable pro-IL-1β. To determine the optimal conditions for inflammasome activation, J774A.1 cells were primed with LPS and stimulated with either ATP or nigericin for 30 and 90 minutes. Morphological changes and pro-IL-1β levels were assessed via inverted phase contrast microscopy and Western blot, respectively (Fig. 1). The untreated cells appeared circular with minimal protrusions. Following LPS priming and 30 minutes of stimulation, cells from both the ATP and nigericin treatment conditions appeared similar in morphology, exhibiting cellular elongation. After 90 minutes, the LPS + nigericin-treated cells underwent further polarization, as indicated by the formation of multidirectional protrusions, shown by the arrows, while the LPS + ATP-treatment condition contained fewer cells displaying a polar phenotype (Fig. 1A). Cells in the LPS + ATP treatment condition possessed a more spherical, bipolar morphology, with few protrusions (Fig. 1A). As expected, the Western Blot performed on cell lysates showed pro-IL-1β in the LPS only treatment condition at 37 kDa (Fig. 1B). Pro-IL-1β was observed for the 30- and 90-mins LPS + nigericin treatment conditions, but not for the LPS + ATP treatment conditions. However, the pro-IL-1β gel bands for the LPS + nigericin treatment conditions were weaker relative to the LPS only control. Based upon the greater morphological changes observed across the treatment time points, and the detection of pro-IL-1β in nigericin-treated cell lysates, nigericin was selected for use as our model-system activator.

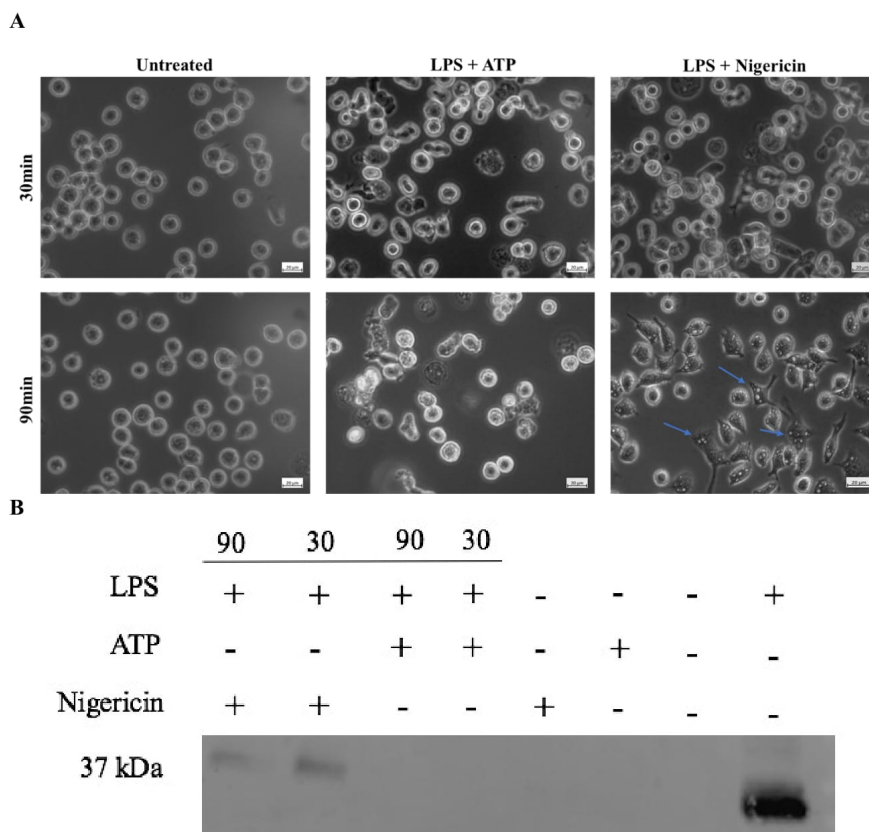
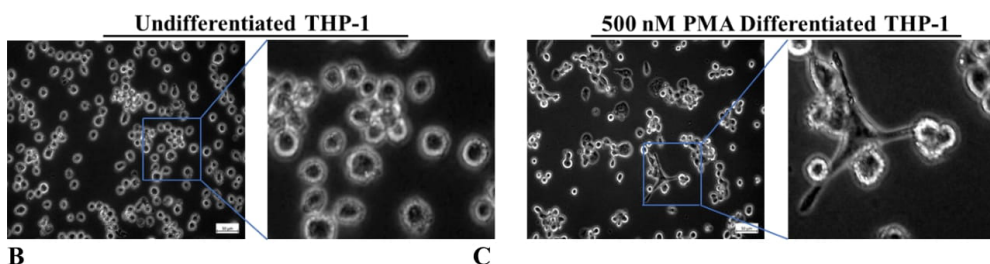


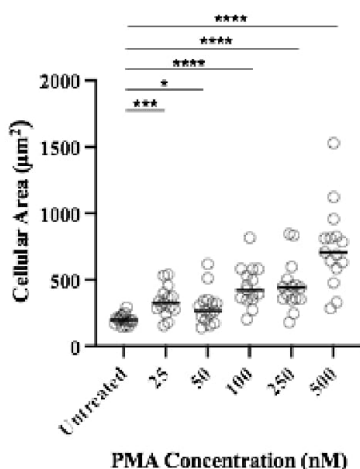
FIG. 1 Short-term nigericin stimulation of LPS-primed J774A.1 cells induces cellular protrusions and pro-IL-1β expression. J774A.1 cells were activated with either 5 mM ATP or 10 µM nigericin subsequent to priming with 0.5 µg/mL LPS for 4 hours. **(A)** 40X magnification inverted phase contrast microscopy images of untreated and LPS-primed, ATP or nigericin-stimulated cells captured after 30 minutes and 90 minutes. Arrows indicate polarized and elongated morphologies. Scale bars = 20 µm. **(B)** Pro-IL-1β detection via Western blot performed on cell lysates.

PMA-differentiated THP-1 cells have a distinct macrophage-like phenotype and become adherent. To differentiate the human monocytic THP-1 cells into a macrophage-like phenotype, undifferentiated THP-1 cells were treated with increasing concentrations of PMA, from 25 nM to 500 nM. After 24 hours, cells were imaged using an inverted phase contrast microscope and the media was removed to observe cellular adherence. With increasing PMA concentration, the THP-1 cells appear to possess larger and elongated, macrophage-like morphologies, as shown by the enlarged images (Fig. 2A). The observed morphological changes were further supported by the relative increase in cellular area and perimeter between the undifferentiated and PMA-differentiated THP-1 cells, semi-quantified using ImageJ (Fig. 2B-C). 24-hour treatment with PMA concentrations above 100 nM induced cell-to-surface adhesion, indicated by the presence of cells following media removal (Fig. 2D). Based on the observed macrophage-like morphology and increased surface adherence, 24 hrs treatment with 500 nM PMA was selected to differentiate THP-1 cells for subsequent experiments.

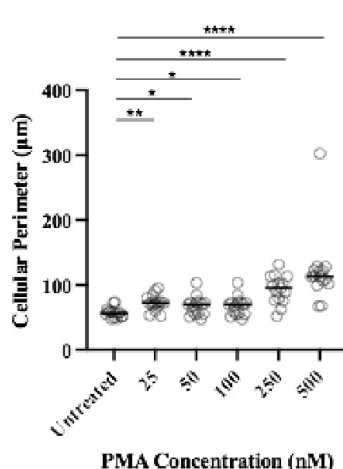
A



B



C



D

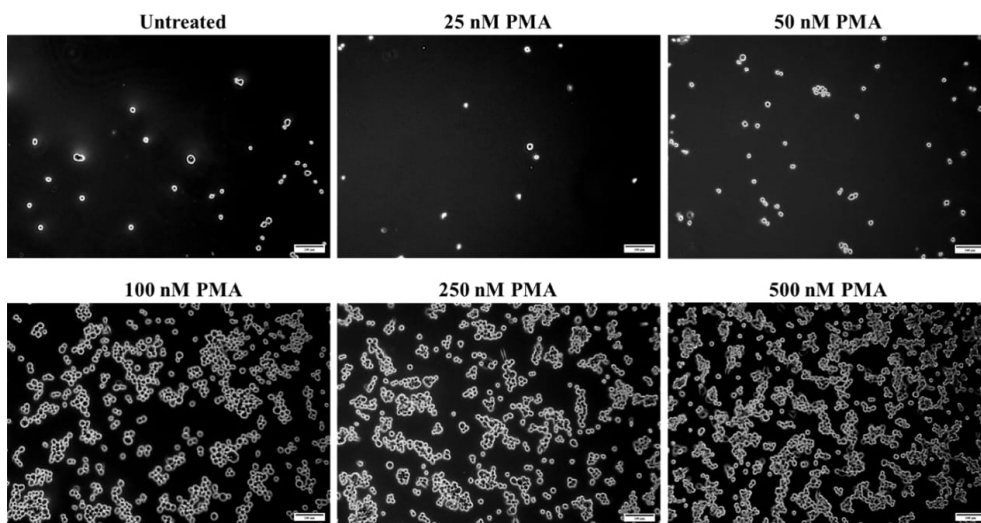
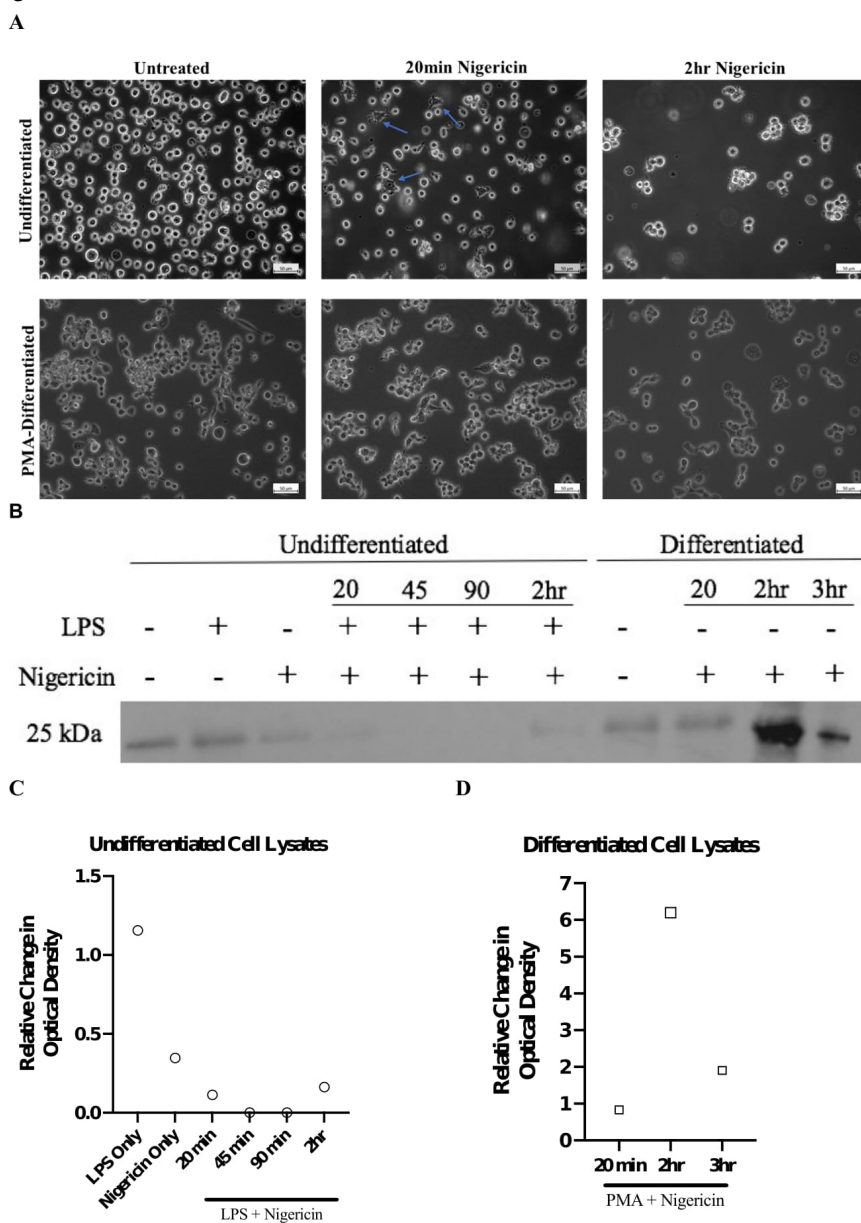


FIG. 2 THP-1 cells were differentiated after 24 hrs of 500 nM PMA treatment. Undifferentiated THP-1 cells were treated with increasing concentrations of PMA (25 nM, 50 nM, 100 nM, 250 nM and 500 nM) for 24 hours and imaged using an inverted phase contrast microscope. **(A)** Representative 20X magnification phase contrast images of the untreated and 500 nM PMA-treated wells. The blue box outline represents the visual field of the enlarged image to the right. Scale bars = 50 µm. **(B-C):** Semi-quantification of cellular area and perimeter of 15 randomly selected cells from each treatment group. Bars represent the median. Significance analyzed via unpaired t-test; *p < 0.05, **p < 0.005, ***p < 0.0005, ****p < 0.00005. **(D)** Representative 20X magnification phase contrast images of all treatment groups with the media removed following incubation for 24 hours. Scale bars = 100 µm.

ASC adaptor protein diminishes in LPS-primed undifferentiated and increases in PMA-differentiated THP-1 cell lysates with nigericin treatment. To establish the presence of the ASC adaptor protein following nigericin treatment in THP-1 cells, LPS-primed undifferentiated and PMA-differentiated THP-1 cells were stimulated with nigericin for up to 2 hrs and 3 hrs, respectively. Following nigericin treatment, inverted phase contrast images were captured, and the cell lysates were assessed for ASC protein levels via Western blot. Few LPS-primed undifferentiated cells appeared to be enlarged, with protrusions observed after 20 mins of nigericin treatment as shown by the arrows (Fig. 3A). However, the PMA-differentiated cells remained phenotypically static following nigericin treatment (Fig. 3A). For the undifferentiated cell lysates, ASC protein was predominantly detected for untreated and LPS only conditions, with reduced band intensities in the nigericin-treated conditions. For the PMA-differentiated cell lysates, ASC band intensity increased between the untreated and the 2 hrs nigericin stimulation conditions, followed by a decrease in band intensity at 3 hrs (Fig. 3B). The Western blot results were further supported by the relative change in ASC band intensity between untreated and experimental conditions, semi-quantified in ImageJ. (Fig. 3C-D). The Western blot data suggest that ASC protein levels decrease in LPS-primed undifferentiated THP-1 cells and increase in PMA-differentiated THP-1 cells, in response to nigericin treatment.

FIG. 3 LPS-treated undifferentiated and PMA-differentiated THP-1 cells possess static phenotypes after nigericin treatment and express ASC independent of nigericin stimulation. LPS-primed undifferentiated (1 µg/ml, 4 hrs) THP-1 cells were treated with 10 µM nigericin for 20 min, 45 min, 90 min, and 2 hrs. PMA-differentiated (500 nM, 24 hrs) THP-1 cells were treated with 10 µM nigericin for 20 min, 2 hrs, and 3 hrs. (A) Representative 20X magnification phase contrast images of untreated, 20 min, and 2 hrs of nigericin treatment. Top: Undifferentiated cells. Arrows indicate larger undifferentiated cells exhibiting protrusions. Bottom: Differentiated cells. Scale bars = 50 µm. (B) Western blot probing for ASC adaptor protein in undifferentiated and differentiated THP-1 cell lysates. (C-D) Densitometric analysis was performed using ImageJ. Relative change in optical intensity represents the intensity ratio between the ASC bands in the experimental and the untreated conditions, for undifferentiated and differentiated cell lysates, respectively.



Increased cell death was observed over time in nigericin-stimulated THP-1 cells. We investigated the time-course profile of THP-1 cell death, to observe the duration-dependent effects of our treatment conditions on downstream pathways related to cell death. We conducted a membrane integrity-based cell viability assay using NucGreen Dead 488 stain with LPS-primed undifferentiated and PMA-differentiated THP-1 monocytes. Following either LPS-priming, or PMA-differentiation, cells were treated with nigericin for 45 mins, 90 mins, and 24 hrs. Fluorescence microscopy of our undifferentiated, stimulated cells displayed an increasing trend in disrupted cell membrane integrity over time. Cell membranes are impermeable to NucGreen Dead-488 DNA stain, and fluorescent detection is facilitated by membrane disruptions. A large increase in fluorescence was observed in the LPS + nigericin conditions relative to the untreated and LPS only control, indicative of plasma membrane disruption (Fig. 4A-F). Increased fluorescence suggesting disrupted membrane integrity was observed as early as 45 mins, indicating that cell death, potentially due to pyroptosis, is occurring prior to the 45 mins time point (Fig. 4D). A similar duration-dependent loss of cell-membrane integrity was observed in the PMA-differentiated, nigericin-stimulated cells (Fig. 4G-K). An increase in fluorescence signal was observed under PMA + nigericin treatment conditions relative to the untreated and PMA-only controls (Fig. 4G-K). Qualitatively, based upon the fluorescence trends, increased treatment times were associated with increased loss of cell membrane integrity (Fig. 4I-K). Similar to the LPS-primed undifferentiated cells, heightened cell death was observed from the 45 mins nigericin treatment (Fig. 2I). The 24 hrs nigericin treatment conditions exhibited the most intense fluorescence signaling, suggesting that cell death occurs in a duration-dependent manner (Fig. 4F, K). These data suggest that increased cell death begins as early as 45 mins and increases afterwards following nigericin treatment for both LPS-primed and PMA-differentiated THP-1 cells.

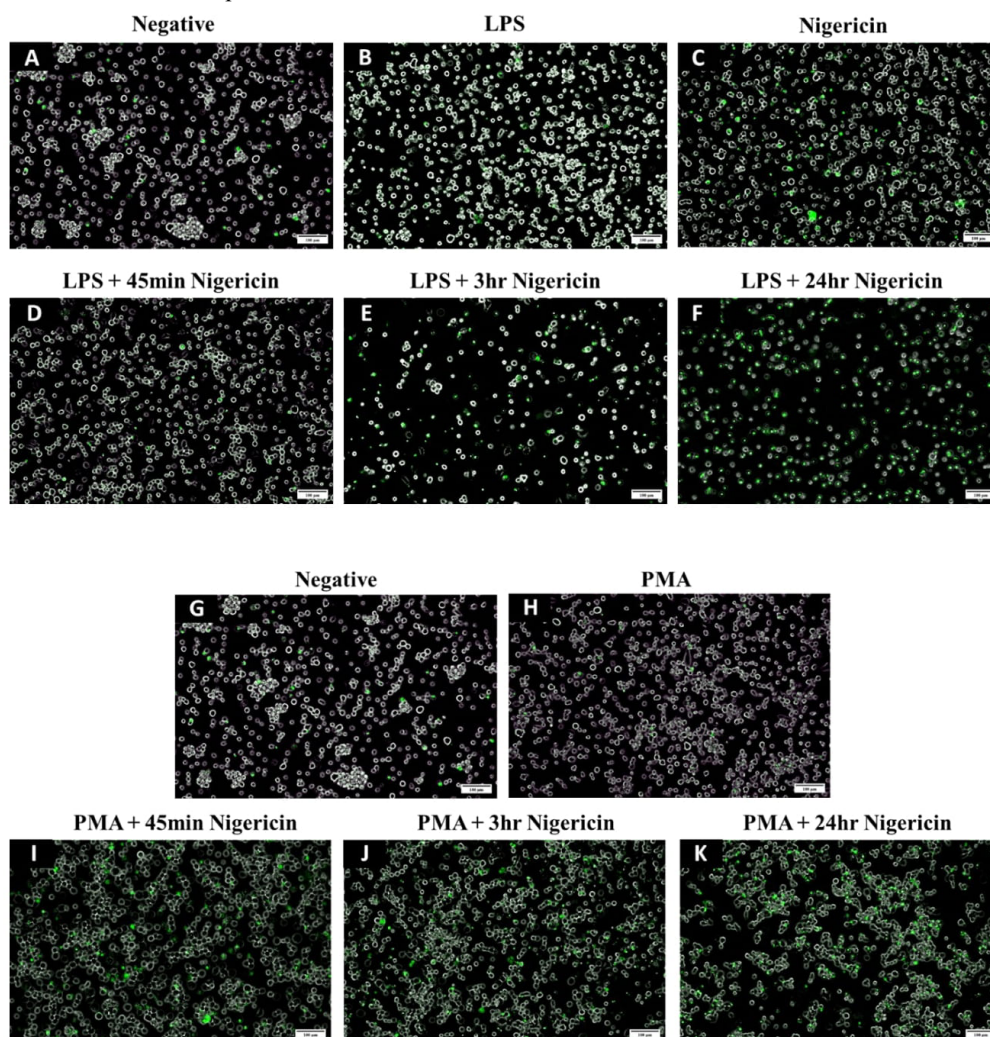


FIG. 4 Nigericin stimulation of LPS-primed undifferentiated and PMA-differentiated THP-1 cells results in increased cell death over time. Overlaid fluorescence and transmitted microscopy images of NucGreen™ Dead 488-stained THP-1 cells. Images were captured at 10X magnification and overlaid using ImageJ. (A-F) Overlay images of LPS-primed undifferentiated (1 $\mu\text{g}/\text{ml}$, 4 hrs) THP-1 cells and (G-K) PMA-differentiated (500 nM, 24 hrs) cells followed by 10 μM nigericin stimulation for 45 min, 3 hrs, and 24 hrs. Scale bar = 100 μm .

DISCUSSION

In this study, we aimed to optimize an *in-vitro* model system to study the canonical activation pathway of the NLRP3 inflammasome in two cell lines. However, we were unsuccessful in identifying robust markers of inflammasome activation. Nonetheless, we were able to replicate previous UJEMI results which observed an upregulation of pro-IL-1 β in J774A.1 cells following LPS stimulation, indicative of successful priming. Additionally, we performed inverted phase-contrast microscopy to compare morphological changes induced by nigericin and ATP. We observed a greater proportion of polar, elongated cells following nigericin treatment relative to ATP, leading us to direct our study towards nigericin-stimulation. Due to our inability to detect mature IL-1 β in J774A.1 cells, we transitioned towards the optimization of a THP-1 human leukemia monocyte cell line model system for NLRP3 inflammasome activation. THP-1 monocytes were differentiated into macrophage-like phenotypes using PMA, and exhibited stable, elongated, and polar morphologies following nigericin stimulation. Both undifferentiated and differentiated THP-1 cells showcased cell death in response to nigericin stimulation. While our results do not demonstrate conclusive activation of the NLRP3 inflammasome, the THP-1 cell line is a promising candidate for further research into the pyroptosis time-course and optimization NLRP3 inflammasome activation assays.

Canonical activation of the NLRP3 inflammasome is thought to involve a two-step process involving PAMPs and DAMPs (2, 3). Macrophages recognize PAMPs such as LPS through interactions with TLR4, inducing the transcription of pro-inflammatory cytokines such as pro-IL-1 β via the NF- κ B pathway (22). In our J774A.1 murine macrophage cells, we detected upregulation of pro-IL-1 β following LPS treatment compared to our untreated, which indicates a successful priming of the NLRP3 inflammasome (Fig. 1B). The second activation signal is provided by PAMPs or DAMPs such as nigericin or ATP, promoting the assembly of the NLRP3 inflammasome (23). Assembly involves the oligomerization of the NLRP3 protein, pro-caspase-1 and the ASC adaptor protein (2). In turn, pro-caspase-1 is auto-proteolytically cleaved into mature caspase-1 which functions to further cleave pro-IL-1 β and full-length GSDMD (2). The cleaved, GSDMD^{N-term} forms pores in the cellular membrane, leading to cytoplasm release and pyroptotic cell death (24). We observed pro-IL-1 β , but not mature IL-1 β , in our LPS-primed, nigericin-stimulated J774A.1 cell lysates at a decreased band intensity compared to the LPS-primed treatment (Fig. 1B). This suggests that upon stimulation with nigericin, the pro-IL-1 β is lost from the cell. One potential mechanism may involve the cleavage of pro-IL-1 β into mature IL-1 β , and the subsequent secretion of IL-1 β via GSDMD^{N-term} pores in the plasma membrane. Therefore, there is a possibility of detecting cleaved IL-1 β in the cell treatment media (9). Following 90-minute nigericin treatment of LPS-primed J774A.1 cells, morphological changes occurred, where cells exhibited multipolar elongation (Fig. 1A). This is similar to previously described morphological characteristics of activated J774A.1 cells, induced by actin-reorganization (25).

Following ATP stimulation of LPS-primed J774A.1 cells, we were unable to detect pro-IL-1 β , which is inconsistent with previous UJEMI results that had obtained pro-IL-1 β after ATP treatment (13-15). This may be due to differences in ATP preparation, which could lead to altered activation of the J774A.1 cells. Without the detection of mature IL-1 β , further research into the appropriate ATP preparation methods is warranted.

The THP-1 cell line has been extensively used as a tool to study various monocyte and macrophage signaling pathways, including the NLRP3 inflammasome (26). THP-1 cells are frequently differentiated into morphologically distinct, adherent, macrophage-like cells through PMA-mediated activation of the PKC pathway (18). Both the undifferentiated and differentiated THP-1 cell types are capable of performing various effector functions of the innate immune system, including activation of the NLRP3 inflammasome (16, 27).

To confirm successful differentiation of THP-1 cells, we analyzed cell morphology and adherence following 24-hour PMA treatments at concentrations ranging from 25-500 nM (Fig. 2). Cell adherence was positively correlated with PMA concentration, with the most adherence seen following 500 nM PMA treatment (Fig. 2D). We also observed the morphological transformation into macrophage-like cells, with elongated, multipolar protrusions observed after 100 nM, 250 nM, and 500 nM PMA treatments (Fig. 2A). Moreover, quantitative and statistical analysis established significant change in cellular area

and perimeter compared to undifferentiated cells (Fig. 2B-C). PMA-differentiation-induced morphological changes are likely associated with upregulated PKC-pathway signaling, and downstream activation of NF- κ B (28).

PMA-differentiation of monocytic THP-1 cells upregulates pro-IL-1 β expression, priming the NLRP3 inflammasome through the PKC-NF- κ B signaling pathway (29). Therefore, we did not perform LPS priming of PMA-differentiated THP-1 cells prior to nigericin stimulation. Both LPS-primed undifferentiated and PMA-differentiated THP-1 cells appeared to possess static cell morphologies in response to nigericin treatment (Fig. 3A). Few undifferentiated cells became elongated, with the majority of the cells resembling unstimulated cells, exhibiting small and circular morphologies. The absence of morphological change in the differentiated THP-1 cells could be due to the cells already possessing an activated macrophage-like phenotype due to the preceding PMA-differentiation.

Next, we analyzed the change in the expression of the ASC adaptor protein in LPS-primed undifferentiated and PMA-differentiated THP-1 cells following nigericin treatment. The ASC adaptor protein provides a scaffold for the oligomerization of the NLRP3 and pro-caspase-1 proteins (2). Following the second activation signal, the ASC protein is dispersed in the cytosol of unstimulated cells and condensed during inflammasome oligomerization (30). We detected ASC in the untreated cell lysates for both undifferentiated and differentiated THP-1 cells via Western blot (Fig. 3B). This may reflect the baseline presence of ASC proteins in the cytosol of monocytes and macrophages. However, following nigericin stimulation, we observed decreased ASC band intensity in LPS-primed, undifferentiated THP-1 cells, and increased ASC band intensity in PMA-differentiated THP-1 cells (Fig. 3C-D). A possibility for the decreased ASC detection in undifferentiated THP-1 cells is its release into the treatment media due to nigericin-induced cell death. Increased ASC detection in PMA-differentiated THP-1 cells may indicate a nigericin-mediated upregulation of ASC. To elucidate the time-course of cell death in undifferentiated and differentiated THP-1 cells, we performed a cell viability assay staining for loss of cell membrane integrity. We observed similar cell death patterns in both LPS-primed undifferentiated and PMA-differentiated THP-1 cells after nigericin treatment (Fig. 4). This indicates that the observed ASC loss in undifferentiated THP-1 cells is unlikely due to inflammasome-mediated cell death. Further research is required to clarify the ambiguity regarding the differential ASC detection between nigericin-treated, undifferentiated and differentiated THP-1 cells. Moreover, the increased levels of fluorescence in our nigericin-only control for the undifferentiated THP-1 cells indicates that cell death may not be induced by NLRP3 inflammasome-mediated pyroptosis. Another explanation for the observed cell death is the capacity of nigericin to form pores in the plasma membrane, inducing lytic cell death and facilitating the binding of NucGreen Dead 488 to DNA.

Conclusions We investigated NLRP3 inflammasome activation in J774A.1 and THP-1 cells. Nigericin stimulation of LPS-primed J774A.1 cells exhibited reduced pro-IL-1 β levels. PMA differentiation of THP-1 cells was optimized at 500nM for 24 hrs. ASC detection post-nigericin treatment increased in differentiated and decreased in LPS-primed, undifferentiated THP-1 cells. Our cell viability assay suggested duration-dependent cell death following nigericin treatment. However, further research is required to associate our findings with NLRP3 inflammasome activation.

Future Directions In our J774A.1 cells, we only probed for intracellular IL-1 β ; a future direction would involve probing for pro- or cleaved-IL-1 β in culture supernatants, either by ELISA or by Western blot following protein concentration. Furthermore, examining different ATP preparation techniques for the activation of J774A.1 cells would help to verify the conflicting results regarding cell morphology and pro-IL-1 β detection between our study and previous UJEMI studies. For optimizing NLRP3 inflammasome activation in THP-1 cells, performing epifluorescence microscopy to observe ASC-speck formation in THP-1 cells following nigericin treatment would provide insight into the different trends in ASC banding observed in our Western blot. Additionally, to confirm whether the observed cell death in our live dead imaging assay is due to inflammasome-induced pyroptosis or LPS/nigericin toxicity, further investigation into detecting markers for NLRP3 inflammasome is required.

We performed epifluorescence microscopy to visualize GSDMD^{N-term} and Western blots probing for cleaved caspase-1 and GSDMD^{N-term} (Supp Fig. S1-S3). However, we were unable to obtain conclusive results. Troubleshooting the caspase-1 and GSDMD^{N-term} Western blots by optimizing the antibody dilution or testing additional nigericin timepoints and concentrations may provide further insight. Additionally, utilizing an inverted confocal microscope may enable visualization of GSDMD^{N-term}.

ACKNOWLEDGEMENTS

We would like to express our sincerest gratitude to Dr. Marcia Graves and Dr. Mihai Cirstea for their guidance and encouragement throughout our project. Additionally, we would like to thank Jade Muileboom and our fellow immunology teams for their advice and technical support. We would also like to thank the Department of Microbiology and Immunology at the University of British Columbia for funding this project.

CONTRIBUTIONS

Each team member contributed an equivalent amount of effort and time towards laboratory work and the production of this project. D.P. contributed to the introduction and the abstract. M.T. wrote the methods and materials and contributed to the making of the figures. J.W. worked on figure design and abstract. A.N worked on the future directions, supplementary figures, and methods. All team members played a part in writing the title, results, discussion, and conclusion.

REFERENCES

1. Medzhitov, R. 2001. Toll-like receptors and innate immunity. *Nature Reviews Immunology* **1**: 135–145.
2. Swanson, K. V., M. Deng, and J. P.-Y. Ting. 2019. The NLRP3 inflammasome: Molecular activation and regulation to therapeutics. *Nature Reviews Immunology* **19**: 477–489.
3. Paik, S., J. K. Kim, P. Silwal, C. Sasakawa, and E.-K. Jo. 2021. An update on the regulatory mechanisms of NLRP3 inflammasome activation. *Cellular & Molecular Immunology* **18**: 1141–1160.
4. Li, Z., J. Guo, and L. Bi. 2020. Role of the NLRP3 inflammasome in autoimmune diseases. *Biomedicine & Pharmacotherapy* **130**: 110542.
5. Lee, J., H. Kim, J. Kim, T. Yook, K. Kim, J. Lee, and G. Yang. 2021. A novel treatment strategy by natural products in NLRP3 inflammasome-mediated neuroinflammation in alzheimer's and parkinson's disease. *International Journal of Molecular Sciences* **22**: 1324.
6. Masters, S. L., E. Latz, and L. A. O'Neill. 2011. The inflammasome in atherosclerosis and type 2 diabetes. *Science Translational Medicine* **3**.
7. Zito, G., M. Buscetta, M. Cimino, P. Dino, F. Bucchieri, and C. Cipollina. 2020. Cellular models and assays to study NLRP3 inflammasome biology. *International Journal of Molecular Sciences* **21**: 4294.
8. Kelly, P., K. G. Meade, and C. O'Farrelly. 2019. Non-canonical inflammasome-mediated IL-1 β production by primary endometrial epithelial and stromal fibroblast cells is NLRP3 and caspase-4 dependent. *Frontiers in Immunology* **10**.
9. Ramachandran, A., B. Kumar, G. Waris, and D. Everly. 2021. Deubiquitination and activation of the NLRP3 inflammasome by UCHL5 in HCV-infected cells. *Microbiology Spectrum* **9**.
10. Molyvdas, A., U. Georgopoulou, N. Lazaridis, P. Hytioglou, A. Dimitriadis, P. Foka, T. Vassiliadis, G. Loli, A. Phillipidis, P. Zebekakis, A. E. Germanis, M. Speletas, and G. Germanidis. 2018. The role of the NLRP3 inflammasome and the activation of IL-1 β in the pathogenesis of chronic viral hepatic inflammation. *Cytokine* **110**: 389–396.
11. Hirano, S., Q. Zhou, A. Furuyama, and S. Kanno. 2017. Differential regulation of IL-1 β and IL-6 release in murine macrophages. *Inflammation* **40**: 1933–1943.
12. Gong, Z., J. Zhou, H. Li, Y. Gao, C. Xu, S. Zhao, Y. Chen, W. Cai, and J. Wu. 2015. Curcumin suppresses NLRP3 inflammasome activation and protects against LPS-induced septic shock. *Molecular Nutrition & Food Research* **59**: 2132–2142.
13. Cortez, S., He, J., Lising, V. 2022. Establishing a J774A.1 Murine Macrophage NLRP3 Inflammasome Model for Examining ShortChain Fatty Acid Suppression. *UJEMI* **27**:1-11.
14. Mansouri Dana, H., Rosen, A., and Tabassi, P. 2022. Towards optimizing ATP-induced activation of the NLRP3 inflammasome in glycolysis inhibited J774A.1 murine macrophages. *UJEMI* **27**:1-13.
15. Sekhon, P., Singh, R., Song, A. 2022. Investigating the role of calcium ion mobilization in NLRP3 inflammasome activation of J774A.1 macrophages and optimizing cell morphology and IL-1 β quantification protocols. *UJEMI* **27**:1-10.
16. Guzova, J. A., M. J. Primiano, A. Jiao, J. Stock, C. Lee, A. R. Winkler, and J. P. Hall. 2019. Optimized protocols for studying the NLRP3 inflammasome and assessment of potential targets of CP-453,773 in undifferentiated THP1 cells. *Journal of Immunological Methods* **467**: 19–28.

17. **Mouasni, S., V. Gonzalez, A. Schmitt, E. Bennana, F. Guillonneau, S. Mistou, J. Avouac, H. K. Ea, V. Devauchelle, J.-E. Gottenberg, G. Chiochia, and L. Fournier.** 2019. The classical NLRP3 inflammasome controls fadd unconventional secretion through microvesicle shedding. *Cell Death & Disease* **10**.
18. **Starr, T., T. J. Bauler, P. Malik-Kale, and O. Steele-Mortimer.** 2018. The phorbol 12-myristate-13-acetate differentiation protocol is critical to the interaction of THP-1 macrophages with salmonella typhimurium. *PLOS ONE* **13**.
19. **Gritsenko, A., S. Yu, F. Martin-Sanchez, I. Diaz-del-Olmo, E.-M. Nichols, D. M. Davis, D. Brough, and G. Lopez-Castejon.** 2020. Priming is dispensable for NLRP3 inflammasome activation in human monocytes *in vitro*. *Frontiers in Immunology* **11**.
20. **Zha, Q.-B., H.-X. Wei, C.-G. Li, Y.-D. Liang, L.-H. Xu, W.-J. Bai, H. Pan, X.-H. He, and D.-Y. Ouyang.** 2016. ATP-induced inflammasome activation and pyroptosis is regulated by AMP-activated protein kinase in macrophages. *Frontiers in Immunology* **7**.
21. **Cullen, S. P., C. J. Kearney, D. M. Clancy, and S. J. Martin.** 2015. Diverse activators of the NLRP3 inflammasome promote il-1 β secretion by triggering necrosis. *Cell Reports* **11**: 1535–1548.
22. **Chen, Z., Y. Liu, B. Sun, H. Li, J. Dong, L. Zhang, L. Wang, P. Wang, Y. Zhao, and C. Chen.** 2014. Polyhydroxylated metallofullerenols stimulate Il-1 β secretion of macrophage through tlr8/myd88/NF-KB pathway and NLRP3 inflammasome activation. *Small* **10**: 2362–2372.
23. **Xia S, Hollingsworth LR 4th, Wu H.** 2020. Mechanism and regulation of gasdermin-mediated cell death. *Cold Spring Harb Perspect Biol* **12**.
24. **Wang, Y., X. Zhu, S. Yuan, S. Wen, X. Liu, C. Wang, Z. Qu, J. Li, H. Liu, L. Sun, and F. Liu.** 2019. TLR4/NF-KB signaling induces GSDMD-related pyroptosis in tubular cells in diabetic kidney disease. *Frontiers in Endocrinology* **10**.
25. **Faust, J. J., A. Balabiyev, J. M. Heddleston, N. P. Podolnikova, D. P. Baluch, T.-L. Chew, and T. P. Ugarova.** 2019. An actin-based protrusion originating from a podosome-enriched region initiates macrophage fusion. *Molecular Biology of the Cell* **30**: 2254–2267.
26. **Zhang, S., Y. Zhang, L. Gan, F. Wei, B. Chai, A. A. Aljaafreh, X. Liu, X. Duan, J. Jiang, X. Wang, M. He, X. Huang, H. Cai, T. Chen, and H. Chen.** 2021. Progesterone suppresses *Neisseria gonorrhoeae*-induced inflammation through inhibition of NLRP3 inflammasome pathway in THP-1 cells and murine models. *Frontiers in Microbiology* **12**.
27. **Yan, C.-Y., S.-H. Ouyang, X. Wang, Y.-P. Wu, W.-Y. Sun, W.-J. Duan, L. Liang, X. Luo, H. Kurihara, Y.-F. Li, and R.-R. He.** 2021. Celastrol ameliorates *Propionibacterium acnes*/LPS-induced liver damage and MSU-induced gouty arthritis via inhibiting K63 deubiquitination of NLRP3. *Phytomedicine* **80**: 153398.
28. **Baxter, E. W., A. E. Graham, N. A. Re, I. M. Carr, J. I. Robinson, S. L. Mackie, and A. W. Morgan.** 2020. Standardized protocols for differentiation of THP-1 cells to macrophages with distinct M(IFN γ +LPS), M(IL-4) and m(il-10) phenotypes. *Journal of Immunological Methods* **478**: 112721.
29. **Lee, J. Y., Y. Kang, H. J. Kim, D. J. Kim, K. W. Lee, and S. J. Han.** 2021. Acute glucose shift induces the activation of the NLRP3 inflammasome in THP-1 cells. *International Journal of Molecular Sciences* **22**: 9952.
30. **Ghait, M., R. A. Husain, S. N. Duduskar, T. B. Haack, M. Rooney, B. Göhrig, M. Bauer, I. Rubio, and S. D. Deshmukh.** 2022. The tlr-chaperone CNPY3 is a critical regulator of nlrp3-inflammasome activation. *European Journal of Immunology* **52**: 907–923.